Transient Response of an Electromagnetic Rail Gun: A Pedagogical Model

by Thomas B. Bahder and John D. Bruno

19980527 015

DTIC QUALITY INSPECTED 4

Army Research Laboratory
Adelphi, MD 20783-1197

Transient Response of an Electromagnetic Rail Gun: A Pedagogical Model

Thomas B. Bahder and John D. Bruno
Sensors and Electron Devices Directorate

Abstract

We present a highly simplified model of an electromagnetic rail gun. The energy source for the gun consists of a rotating magnetic dipole moment positioned at the center of a stator coil. The dipole moment is free to rotate about an axis normal to the stator coil's axis, inducing a current in the rail gun stator circuit, and thereby propelling the projectile. The system's dynamical behavior is described by three nonlinear coupled ordinary differential equations, involving time-dependent functions representing the armature's position, the stator circuit's current, and the dipole moment's angular position. We numerically solve this system of differential equations and plot the solutions versus time. The results exhibit a complicated dynamics due to the interaction of the electrical and mechnical degrees of freedom.

Contents

Figures

Table

1. Introduction

The electromagnetic rail gun (EMRG) has been proposed as a viable technology for launching projectiles at speeds over 2500 m/s. A small-scale EMRG was reported a number of years ago [1]; however, the physics of the propulsion mechanism was sufficiently complex that it was still being discussed in the literature 10 years later [2–4].

For nearly a decade, the Army has pursued the development of a larger EMRG for applications in armored vehicles (for a review of this work, see McCorkle [5]). Recently, the technical feasibility of developing a full-scale EMRG, capable of launching a 6-kg projectile, has been questioned at a fundamental level [5] by the Technical Director of the Missile Command (MICOM), W. C. McCorkle.* We have attempted to assess the merits of issues raised in McCorkle's critique, and in so doing, have found it useful to construct a simplified model of the EMRG. The purpose of this report is to document this work.

In the following, we formulate a pedagogical model of an EMRG. The purpose of the model is to provide a simple context within which the basic operating principles of an EMRG can be studied, without many of the complications of the real system. Such a model is useful because it permits us to develop an intuition for much of the physics involved in the real EMRG.

The essence of our EMRG model is a rotating magnetic dipole, which constitutes the system's rotor. This magnetic dipole is inductively coupled to the stator coil that feeds current into the rails of the EMRG. The model is described by three coupled nonlinear ordinary differential equations in time. In section 1, we describe our simplified model of the EMRG. In section 2, we derive the dynamical equations that govern the time evolution of the EMRG system. In section 3, we numerically solve these equations, for two different initial conditions. Finally, we summarize our conclusions in section 4.

---

*The delivered energy density is believed to decrease with increasing total machine weight, assuming that the rail gun length is constant. This constraint is a requirement for applications in armored vehicles. The total machine weight is taken to be the power supply, electronics, and all supporting mechanical equipment.

2. The Model

Figure 1 shows a schematic representation of a simplified EMRG. Our conceptual model of the EMRG consists of a rotating hard magnet with a magnetic moment $\mathbf{M}$ located at the center of a fixed stator coil. The moment is free to rotate about an axis normal to the stator coil's symmetry axis. This rotating magnetic moment plays the role of the field windings on the rotor that is used to power the EMRG. The rotating magnetic moment $\mathbf{M}$ induces an electromotive force (emf) in the surrounding stator coil (single turn), which has an area $A = \pi a^2$, where a is the coil's radius. We call the axis of the stator coil the z-axis, and assume that the magnetic moment $\mathbf{M}$ has a large mechanical moment of inertia $\mathcal{I}$ about an axis perpendicular to this z-axis. At times $t \leq 0$, the rotor (magnetic moment) has a large angular velocity $d\theta/dt = \omega = \omega_0$, and we assume that the stator circuit is open so that there is zero current in the stator circuit, $I = 0$. At $t = 0$, we close the stator circuit, and the induced emf creates a current I for times $t > 0$. The current I in the stator circuit, as shown in figure 1, creates a magnetic field $\mathbf{B}$ perpendicular to the plane of the paper. The railgun armature, shown as the black bar in figure 1, conducts the current I, and is free to move in the x-direction. This armature is in physical contact with the projectile, accelerating it from its initial position at the breech of the gun's barrel to its muzzle. By the Lorentz force law, a current element of length $d\mathbf{l}$ in the armature experiences a magnetic force

$$d\mathbf{F} = I d\mathbf{l} \times \mathbf{B}. \tag{1}$$

The current I is, of course, coupled to the rotor with the magnetic moment $\mathbf{M}$. The rotational kinetic energy of the rotor at $t = 0$ is the only energy stored in the system for times $t < 0$. For times $t > 0$, after the stator circuit switch is closed, some of this rotor kinetic energy goes into kinetic energy of the launch package (armature + projectile) of mass m, Joule heating of the stator circuit, and stored energy in the magnetic field of the stator circuit.[*]

---

[*]The rotor kinetic energy also goes into radiative energy loss, since the rotating magnetic moment produces a time-varying magnetic field. However, the power associated with this radiative loss is negligible for all rotational frequencies of interest.

Figure 1.
Schematic of
electromagnetic
rail gun model.
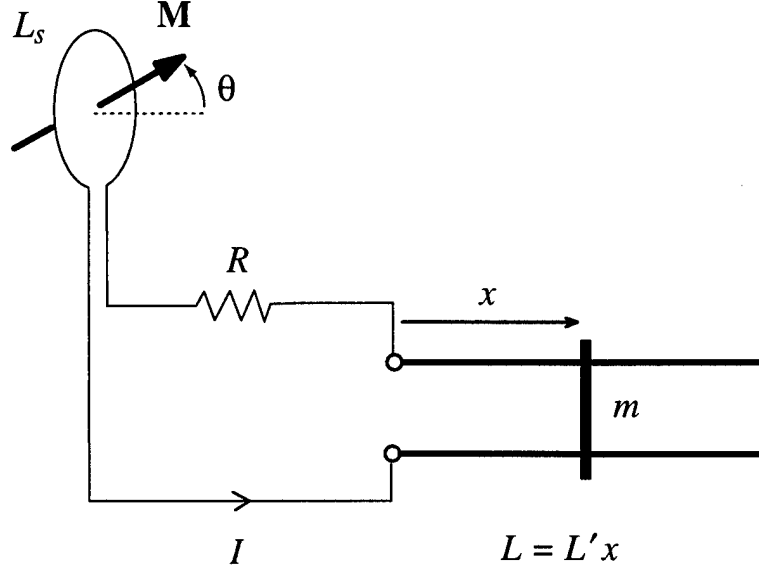
We now derive the differential equations that describe the dynamics of this system. We take the hard magnet to be a simple magnetic dipole moment $\mathbf{M}$, located at the center of the stator coil. The $\mathbf{B}_M$ field of this dipole moment is given by

$$\mathbf{B}_M = \frac{\mu_0}{4\pi}\left[-\frac{\mathbf{M}}{r^3} + \frac{3(\mathbf{M}\cdot\mathbf{r})\mathbf{r}}{r^5}\right], \qquad (2)$$

where $\mathbf{r}$ is the vector from the point dipole $\mathbf{M}$ to the field point. The hard magnetic moment is intended to represent the effects of real currents in the generator's field windings. Since the field-winding circuit dynamics are not included in the present model, we assume that the hard magnet is turned on at some time before $t = 0$, and retains a constant magnetic moment for $t \geq 0$. Hence, for $t \geq 0$, $\mathbf{M}$ has the functional form

$$\mathbf{M}(t) = M_0\left(\cos\theta(t)\,\hat{\mathbf{z}} + \sin\theta(t)\,\hat{\mathbf{x}}\right), \qquad (3)$$

where M_0 is a constant, $\hat{\mathbf{z}}$ and $\hat{\mathbf{x}}$ are unit vectors, and $\theta(t)$ is the angular position of the dipole. At a given time t, the vector $\mathbf{M}$ makes an angle θ with the z-axis, which coincides with the axis of the stator coil. The magnetic field flux density passing though the plane of the stator coil ($z = 0$) is given by

$$\mathbf{B}_M \cdot \hat{\mathbf{z}} = -\frac{\mu_0}{4\pi}\frac{M_0\cos\theta}{\rho^3}, \qquad (4)$$

3

where $\rho^2 = x^2 + y^2$, and the center of the stator coil is taken to coincide with $z = 0$, the origin of coordinates in the x-y plane. The flux passing through the area occupied by the stator coil, given by $\rho \leq a$, is the integral of equation (4) over this region. This integral is divergent, because there is a Dirac delta function contribution that is missing from the expression for the dipole field given in equation (2). However, the total magnetic flux passing through the plane of the stator coil is $\Phi_{in} + \Phi_{out} = 0$, where Φ_{in} is the flux passing through the area occupied by the stator coil, and Φ_{out} is the flux passing through the plane of the coil for $\rho \geq a$. Consequently, we can find the flux passing through the stator coil by integrating the flux density in equation (4) over the region $\rho \geq a$. We obtain

$$\Phi_{in} = \frac{\mu_0 M_0 \cos \theta}{2a} = k M_0 A \cos \theta, \tag{5}$$

where

$$kA = \frac{\mu_0}{2a}. \tag{6}$$

We assume that the stator coil has a self-inductance L_s and that there is a small resistance R in the stator circuit. The rails of the EMRG have a self-inductance

$$L = L'x, \tag{7}$$

which depends on the position x of the launch package mass m. The parameter L' is the self-inductance per unit length of the rails. For two straight parallel rails of circular cross section, each of radius b, and separated by a distance h, we have the approximate form [6]

$$L' = \frac{\mu_0}{4\pi} \left(1 + 4 \log \frac{h}{b} \right). \tag{8}$$

Note that L' is a geometrical constant that is independent of the launch package position x and time t. We ignore in this model the small increase in stator circuit resistance as x increases.

4

3. Derivation of the Dynamical Equations

The EMRG consists of a magnetic moment $\mathbf{M}$ coupled inductively to the stator coil. The stator coil is coupled to the rails of the EMRG by the current I. We assume that the flux of the magnetic field due to the current I in the rails does not couple to the stator coil or to the magnetic moment $\mathbf{M}$. Hence, the rails form an isolated magnetic system.

Within the quasi-static approximation, we consider the free energy of the magnetic system [6]

$$\delta\mathcal{F} = -\mathcal{S}\delta T + \int \mathbf{H} \cdot \delta\mathbf{B} \, dV, \tag{9}$$

where $\mathcal{S}$ is the total entropy of the system, T is the temperature (assumed uniform), and the integration is over the volume where the fields are nonzero. The free energy $\mathcal{F}$ is the work that must be done on the system by external electromotive forces to set up the magnetic fields $\mathbf{H}$ and $\mathbf{B}$. Assuming that all conductors and the surrounding medium in the EMRG have a linear relation between $\mathbf{B}$ and $\mathbf{H}$,

$$\mathbf{B} = \mu\mathbf{H}, \tag{10}$$

equation (9) can be integrated from an initial thermodynamic state $R_0 = (T, \mathbf{B} = 0)$ to a final state $R = (T, \mathbf{B})$. We obtain*

$$\mathcal{F} = \mathcal{F}_0(T) + \frac{1}{2}L_M I_M^2 + L_{MS}I_M I + \frac{1}{2}L_S I^2 + \frac{1}{2}L'x I^2, \tag{11}$$

where $\mathcal{F}_0(T)$ is the free energy $\mathcal{F}$ in state R_0, which depends only on temperature.

---

*When the linear assumption in equation (10) is made, with a temperature-independent permeability, the free energy $\mathcal{F}$ can be written as a sum of the work done to set up the magnetic system, plus a temperature-dependent constant $\mathcal{F}_0(T)$. In this case, the currents in the system do not depend on the thermodynamic state; i.e., they do not depend on temperature. We can then neglect the constant $\mathcal{F}_0(T)$ and speak of the energy of the system. We do this in the ensuing discussion. The resulting quantity, $\mathcal{F} - \mathcal{F}_0(T)$, is then equal to the coenergy, $W = \int_V \int_{R_0}^{R} \mathbf{B} \cdot \delta\mathbf{H} \, dV$. See, for example, Fitzgerald et al [7].

The second term represents the energy required to set up the hard magnetic moment **M**, in the absence of the other parts of the system. Here we treat the hard magnetic moment as a simple self-inductance L_M carrying a current I_M. Since we treat the magnetic moment as constant, the second term in equation (11) is a constant. The fourth term in equation (11) is the energy required to set up the magnetic field due to the current in the stator coil, I, in the absence of the rest of the system.

The third term in equation (11) is the energy of interaction between the magnetic moment **M** and the stator coil. The interaction is given in terms of the mutual inductance L_{MS}, which depends on the relative orientation of the magnetic moment and the stator coil. Consideration of the interaction of two circuits (one circuit representing the magnetic moment **M** and the other circuit representing the stator coil) allows us to write the interaction term as

$$L_{MS}I_M I = +\mathbf{M} \cdot \mathbf{B}_s = M_0 B_s \cos\theta = M_0 \frac{\mu_0 I}{2a} \cos\theta. \tag{12}$$

The fifth term in equation (11) is the magnetic energy required to set up the magnetic field of the rails. Note that we have assumed that the rails are isolated magnetically from other parts of the system, so that there are no interaction terms in $\mathcal{F}$ between the rails and other parts of the system: i.e., the flux of the magnetic field from the rails does not couple to the stator coil or to the magnetic moment.

The magnetic energy in equation (11) is a function of two currents, I and I_M, and two coordinates, θ and x. Derivatives of the energy with respect to the coordinates, at constant currents, give the generalized forces on the system [6]. Here, these derivatives give the force on the mass m and the torque on the magnetic moment:

$$m\ddot{x} = \left(\frac{\partial \mathcal{F}}{\partial x}\right)_{I,I_M}, \tag{13}$$

$$\mathcal{I}\ddot{\theta} = \left(\frac{\partial \mathcal{F}}{\partial \theta}\right)_{I,I_M}. \tag{14}$$

The derivatives given in equations (13) and (14) lead to two dynamical equations,

$$m\ddot{x} = \frac{1}{2}L'I^2, \tag{15}$$

$$\mathcal{I}\ddot{\theta} = -\frac{\mu_0 M_0}{2a}I\sin\theta. \tag{16}$$

6

The above two equations could be obtained directly from Newton's laws of motion and the Lorentz force, equation (1).

The third dynamical equation comes from consideration of the electric fields in the stator circuit, in the presence of magnetic flux passing through the circuit. We derive Ohm's law for this circuit in the presence of a magnetic field. The externally induced emf in the stator cicuit, which does work on the circuit, is due to the *external* magnetic flux passing through this circuit, caused by the rotating magnetic moment **M**. The power dissipated in the stator circuit, $\mathcal{E}I$, is given in terms of the externally induced emf $\mathcal{E}$:

$$\mathcal{E}I = I^2 R + \frac{d}{dt}\left(\frac{1}{2}L_S I^2\right) + \frac{d}{dt}\left(\frac{1}{2}L I^2\right) + \frac{d}{dt}\left(\frac{1}{2}m\dot{x}^2\right), \qquad (17)$$

where L is given by equation (7). From equation (17), this externally induced emf is given by*

$$\mathcal{E} = IR + L_S \dot{I} + L'\left(x\dot{I} + \frac{1}{2}\dot{x}I\right) + \frac{m\dot{x}\ddot{x}}{I}. \qquad (18)$$

On the other hand, the externally induced emf in the stator circuit is associated with a nonconservative electric field $\mathbf{E}_M$, due to the changing field $\mathbf{B}_M$, where $\mathbf{B}_M$ is the field of the magnetic moment given by equation (4). These fields are related by the Maxwell equation

$$\operatorname{curl}\mathbf{E}_M = -\frac{\partial \mathbf{B}_M}{\partial t}. \qquad (19)$$

The externally induced emf in the stator circuit can be written in terms of the line integral of $\mathbf{E}_M$ around the stator circuit,

$$\mathcal{E} = \oint \mathbf{E}_M \cdot d\mathbf{l} = -\frac{d}{dt}\int \mathbf{B}_M \cdot d\mathbf{S} = -\frac{d\Phi_{in}}{dt} \qquad (20)$$

$$= kM_0 A\dot{\theta}\sin\theta, \qquad (21)$$

where Φ_{in} is given by equation (5).

---

*The externally induced emf is not the total emf. The total emf is given by the line integral around the stator circuit, $\oint \mathbf{E}_{total} \cdot d\mathbf{l}$, where $\mathbf{E}_{total}$ is the total nonconservative electric field in the stator circuit. The externally induced emf is the line integral of the electric field $\mathbf{E}_M$ associated with the *external* magnetic flux through the stator circuit, due to the magnetic moment **M**. The electric field $\mathbf{E}_M$ is related to the magnetic field $\mathbf{B}_M$ of the magnetic moment by equation (19).

Using the emf in equation (21) in equation (18), we obtain the third dynamical equation:

$$IR + L_S \dot{I} + L' \left(x\dot{I} + \frac{1}{2}\dot{x}I \right) + \frac{m\dot{x}\ddot{x}}{I} - kM_0 A \dot{\theta} \sin\theta = 0. \qquad (22)$$

We can put equation (22) into a more symmetrical form by using equation (15) to eliminate $\ddot{x}$, giving the third dynamical equation as

$$IR + L_S \dot{I} + L'(x\dot{I} + \dot{x}I) - kM_0 A \dot{\theta} \sin\theta = 0. \qquad (23)$$

Equations (15), (16), and (23) are a complete set of dynamical equations for the quantities $x(t)$, $I(t)$, and $\theta(t)$. These equations are nonlinear differential equations of second order in $x(t)$ and $\theta(t)$ and first order in $I(t)$. Consequently, as discussed above, we take the initial conditions to be

$$
\begin{aligned}
I(0) &= 0, & (24) \\
x(0) &= 0, & (25) \\
\dot{x}(0) &= 0, & (26) \\
\theta(0) &= 0, & (27) \\
\dot{\theta}(0) &= \omega_0, & (28)
\end{aligned}
$$

where ω_0 is the initial angular velocity of the rotor at $t = 0$.

The goal of the EMRG is to launch a projectile with as high a kinetic energy as possible, subject to certain constraints on the acceleration to prevent material failures. To this end, we want to maximize the transfer of the initial rotor energy,

$$U_0 = \frac{1}{2}\mathcal{I}\omega_0^2, \qquad (29)$$

into launch package kinetic energy,

$$K_0 = \frac{1}{2}m\dot{x}^2(t_f), \qquad (30)$$

where $\dot{x}^2(t_f)$ is the speed of the launch package at the gun's muzzle, where the time t_f is given by $x(t_f) = L_g$. Consequently, we want to maximize the quantity

$$\eta = \frac{K_0}{U_0} = \frac{\kappa}{\gamma}\tilde{x}'(\tilde{t}_f), \qquad (31)$$

8

where the dimensionless quantities $\tilde{x}$ and $\tilde{t}$ are given by $\tilde{x} = x/L_g$, and $\tilde{t} = \omega_0 t/(2\pi)$, with $\tilde{x}' = d\tilde{x}/d\tilde{t}$. Equation (31) gives the fraction of rotor kinetic energy that is transferred into launch package kinetic energy. Solution of the system of differential equations in equations (15), (16), and (23) allows calculation of the dependence of η on system parameters.

4. Numerical Solution of the Differential Equations

The nonlinear nature of the dynamical equations (15), (16), and (23) makes it unlikely that we can find a closed-form analytic solution. Therefore, we solve these equations numerically, subject to the initial conditions in equation (28).

For convenience, we first rewrite equations (15), (16), and (23) in terms of dimensionless variables:

$$\tilde{x} = \frac{x}{L_g}, \tag{32}$$

$$\tilde{I} = \frac{R}{kM_0A\omega_0 I}, \tag{33}$$

$$\tilde{\theta} = \frac{\theta}{2\pi}, \tag{34}$$

$$\tilde{t} = \frac{\omega_0}{2\pi}t, \tag{35}$$

where L_g is the length of the railgun, and time is measured in units of $2\pi/\omega_0$, which is the period of rotation of the rotor at $t = 0$.

In terms of the dimensionless variables $\tilde{x}$, $\tilde{I}$, $\tilde{\theta}$, and $\tilde{t}$, the dynamical equations (15), (16), and (23) become

$$2\kappa\,\tilde{x}'' - \beta\tilde{I}^2 = 0, \tag{36}$$

$$\gamma\,\tilde{\theta}'' + \tilde{I}\sin(2\pi\tilde{\theta}) = 0, \tag{37}$$

$$\tilde{I} + \alpha\,\tilde{I}' + \beta\left(\tilde{x}'\,\tilde{I} + \tilde{x}\,\tilde{I}'\right) - \tilde{\theta}'\sin(2\pi\tilde{\theta}) = 0, \tag{38}$$

where the primes denote differentiation with respect to the dimensionless time, and the dimensionless parameters α, β, γ, and κ are defined as

$$\alpha = \frac{L_S}{R}\frac{\omega_0}{2\pi}, \tag{39}$$

$$\beta = \frac{L'L_g}{R}\frac{\omega_0}{2\pi}, \tag{40}$$

$$\gamma = \frac{2U_0}{E_0}, \tag{41}$$

$$\kappa = \frac{2K_0}{E_0}, \tag{42}$$

where U_0 is the initial rotational kinetic energy of the rotor,

$$U_0 = \frac{1}{2}\mathcal{I}\omega_0^2, \tag{43}$$

and K_0 is a characteristic kinetic energy associated with the linear translation of the launch package mass m:

$$K_0 = \frac{1}{2}m\left[\frac{L_g\omega_0}{2\pi}\right]^2. \tag{44}$$

In equation (42), E_0 is a characteristic energy scale in the problem given by

$$E_0 = \frac{V_0^2}{R}\frac{2\pi}{\omega_0}, \tag{45}$$

where V_0 is a characteristic emf induced in the stator circuit

$$V_0 = kM_0A\omega_0. \tag{46}$$

Each of the dimensionless parameters α, β, γ, and κ has a simple physical interpretation. The parameter α is a measure of the ratio of the inductive time constant, L_S/R, to the initial (mechanical) rotation period of the rotor, $2\pi/\omega_0$. The parameter β is a measure of the inductive time constant of the rails, $L'L_g/R$, to the initial rotation period of the rotor. The parameter γ is a measure of the initial rotational kinetic energy of the rotor, and the parameter κ is proportional to the characteristic kinetic energy K_0.

We integrate equations (36) to (38) numerically using the values of α, β, γ, and κ given in table 1, and subject to the initial conditions in equation (28). Initially, the angular velocity of the rotor is ω_0.

The (dimensionless) launch package position $\tilde{x}$ is plotted as a function of (dimensionless) time $\tilde{t} = \omega_0 t/(2\pi)$ in figure 2. The $\tilde{t}$ axis corresponds to

Table 1. Values of dimensionless parameters.

Parameter	Value
α	0.36
β	0.36
γ	0.307
κ	0.0176

Figure 2. Plot of position $\tilde{x}(\tilde{t})$ versus $\tilde{t}$ for initial conditions $\theta(0) = 0$ (solid curve) and $\theta(0) = \pi/2$ (dashed curve).
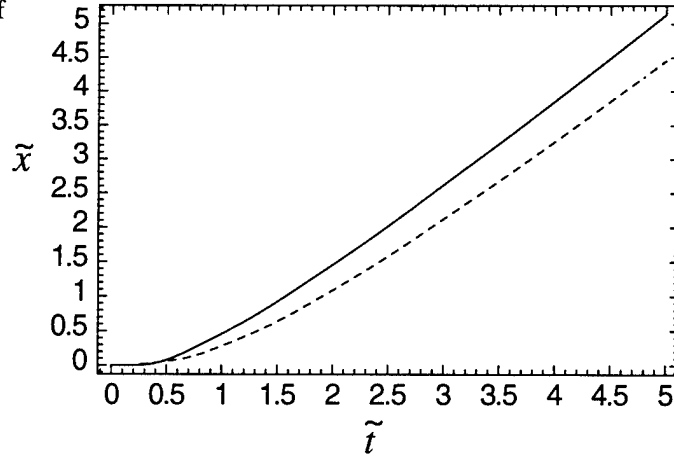

measuring time in periods of revolution at $t = 0$. The position $\tilde{x}$ is generally an increasing function of time $\tilde{t}$, as expected. However, the plot starts out rather flat near $\tilde{t} = 0$, and at approximately $\tilde{t} = 0.3$, there is an upturn. The figure shows $\tilde{x}$ versus $\tilde{t}$ for two initial conditions: $\theta(0) = 0$ (solid curve) and $\theta(0) = \pi/2$ (dashed curve). At any time t, for $\theta(0) = \pi/2$, the armature has not traveled as far as for $\theta(0) = 0$.

For $\tilde{t} > 1.5$, the dimensionless launch package position $\tilde{x}$ appears to be a straight line on this scale; however, there is in fact a slight ripple, which shows up clearly in figure 3, which shows the dimensionless velocity of the launch package $\tilde{x}'(\tilde{t})$ plotted versus time $\tilde{t}$, for the initial conditions $\theta(0) = 0$ (solid curve) and $\theta(0) = \pi/2$ (dashed curve). This velocity plot clearly shows ripples associated with the acceleration of the launch package, which is proportional to $\tilde{I}^2$ (see eq (15)).

Unlike in some actual EMRG designs, in this model there is an alternating current in the stator coil induced by the magnetic moment. However, the (dimensionless) acceleration $\tilde{x}(\tilde{t})''$ is proportional to the square of the current $\tilde{I}^2$, and hence there are no essential differences in the operating principles between ac and dc designs. Note, however, that if we want to maximize the velocity of the armature, we would choose to close the switch on the stator coil at a time that coincides with the $\theta = 0$ position of the rotor. The difference in the velocities of the armature for the initial conditions $\theta(0) = 0$ and $\theta(0) = \pi/2$ depends in a complicated way on the parameters in the problem. Furthermore, the armature containing the projectile cannot leave the gun muzzle (break the stator circuit) at an arbitrary time, since there

12

Figure 3. Plot of velocity $\tilde{x}'(\tilde{t})$ versus $\tilde{t}$ for initial conditions $\theta(0) = 0$ (solid curve) and $\theta(0) = \pi/2$ (dashed curve).
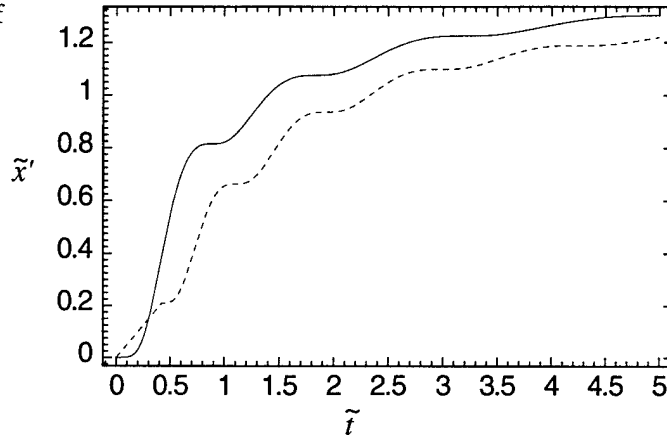
is typically a significant current in the stator circuit, and this would lead to arcing problems in practice. The requirement of zero stator current before the stator circuit is broken (or the switching of stator circuit current) is an additional constraint in a real EMRG system.

The fraction of rotor kinetic energy that is transferred to the launch package, given by η in equation (31), is $\eta = 0.070$ and $\eta = 0.063$, for the initial conditions $\theta(0) = 0$ and $\theta(0) = \pi/2$, respectively, and time $\tilde{t}_f = 3.0$. However, the value of η depends in a complex way on the system parameters and on the precise choice of time $\tilde{t}_f$ (see fig. 3).

The (dimensionless) acceleration $\tilde{x}''(\tilde{t})$ versus $\tilde{t}$ is shown in figure 4. Since the acceleration is proportional to the square of the current, the acceleration peaks at the peak magnitude of the current (see eq (15)).

However, the peak in the stator current lags the emf induced in the stator circuit by a variable amount of phase through the ac cycle, in contrast to a simple steady-state inductive resistive circuit, where the current lags the voltage across the inductor by $\pi/2$. The emf induced in the stator circuit, $\mathcal{E}$, given in equation (18), is given in dimensionless form by

$$\tilde{V}(\tilde{t}) = \frac{\mathcal{E}}{V_0} = \tilde{I} + \alpha \tilde{I}' + \beta \left(\tilde{x}' \tilde{I} + \tilde{x} \tilde{I}' \right). \tag{47}$$

Figure 5 shows the voltage-current phase relations for the initial condition $\theta(0) = 0$. Note that closing the stator circuit switch at $\theta = 0$ corresponds to closing the switch at minimum voltage. The variable phase through the ac cycle between the current and the induced voltage is due to the particular

Figure 4. Plot of
acceleration
$\tilde{x}''(\tilde{t})$ versus $\tilde{t}$
for initial
conditions
$\theta(0) = 0$ (solid
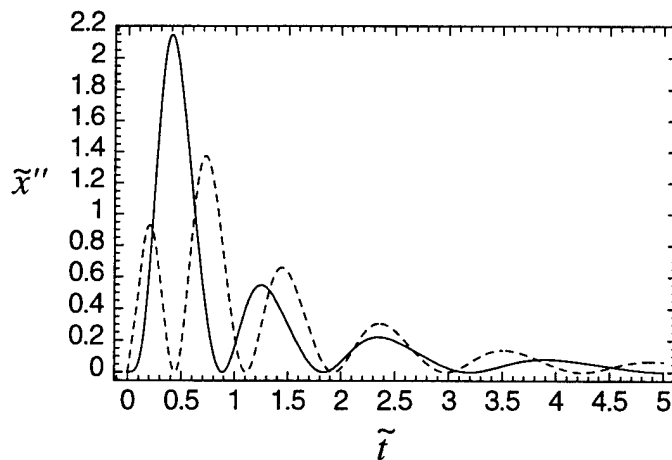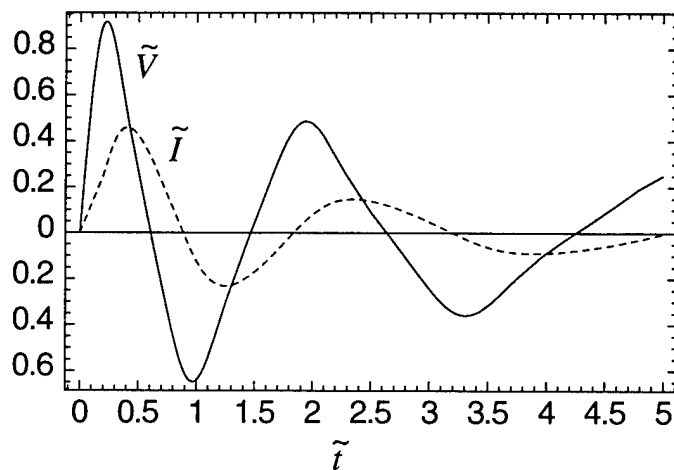curve) and
$\theta(0) = \pi/2$
(dashed curve).

Figure 5. Plot of
voltage $\tilde{V}$ and
current $\tilde{I}(\tilde{t})$ in
stator circuit
versus $\tilde{t}$, for
initial condition
$\theta(0) = 0$.

initial conditions and to the variable coupling of the stator circuit to the launch package mass as the mass m moves down the rails. The detailed phase relationship between the current and voltage depends in a sensitive way on the values of the parameters in the problem.

A similar complicated phase relationship exists for the initial condition $\theta(0) = \pi/2$, which is shown in figure 6.

During the firing of the EMRG, the kinetic energy of the rotor goes into the magnetic field energy of the stator circuit, Joule heating, and the kinetic energy of the launch package. Consequently, on average, the rotor kinetic energy decreases. However, this process is nontrivial. Figure 7 shows the

14

Figure 6. Plot of voltage $\tilde{V}$ and current $\tilde{I}(\tilde{t})$ in stator circuit versus $\tilde{t}$, for initial condition $\theta(0) = \pi/2$.
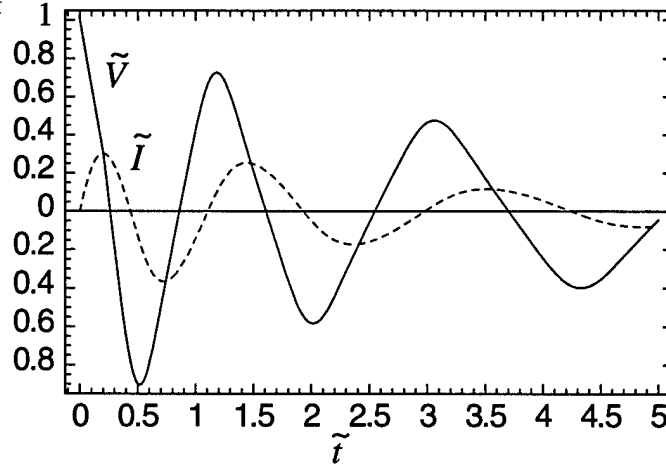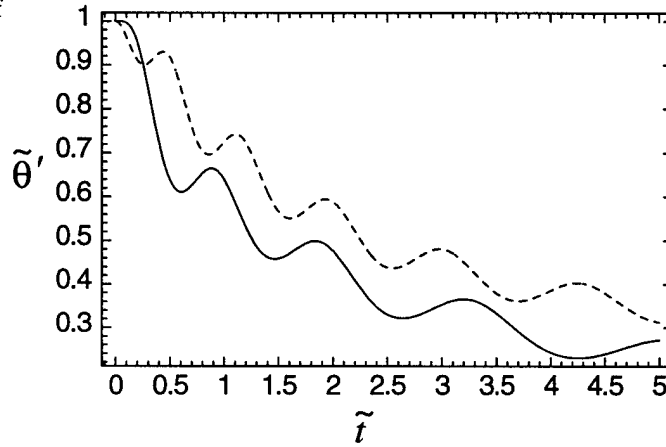
Figure 7. Plot of rotor angular velocity $\tilde{\theta}'(\tilde{t})$ versus $\tilde{t}$, for initial conditions $\theta(0) = 0$ (solid curve) and $\theta(0) = \pi/2$ (dashed curve).

angular velocity of the rotor for the two initial conditions, $\theta(0) = 0$ and $\theta(0) = \pi/2$. Consider the solid curve for initial condition $\theta(0) = 0$. With increasing time, the rotor angular velocity initially decreases, then it increases (near $\tilde{t} = 0.9$), and again decreases. The increase in rotor angular velocity is a consequence of the coupling of the rotor to the stator circuit. During the shot, starting at $\tilde{t} = 0$, energy from the rotor is transferred to the stator circuit, thereby decreasing the rotor angular velocity. At approximately $\tilde{t} = 0.6$, some of the energy from the stator circuit is transferred back to the rotor, causing the rotor to speed up. The transfer of energy from the stator circuit back to the rotor occurs only for a short period of time, from approximately $\tilde{t} = 0.6$ to $\tilde{t} = 0.9$. At time $\tilde{t} = 0.9$, energy is again transferred from the rotor

15

to the stator circuit. The process continues with a decreasing amplitude of oscillation with time.

The behavior of the system for the initial condition $\theta(0) = \pi/2$ is similar to the behavior for the initial condition $\theta(0) = 0$. However, for $\theta(0) = \pi/2$, the phase relationships are different, and the rotor has not lost as much energy for times later than $\tilde{t} \approx 0.25$.

Figure 8 shows the angular acceleration of the rotor, which is proportional to the torque acting on the rotor. Clearly, the torques on the rotor have a complicated time dependence for both initial conditions considered. Such complex phase relationships must be carefully considered in the design of any practical EMRG.

Figure 8. Plot of rotor angular acceleration $\tilde{\theta}''(\tilde{t})$ versus $\tilde{t}$, for initial conditions $\theta(0) = 0$ (solid curve) and $\theta(0) = \pi/2$ (dashed curve).

16
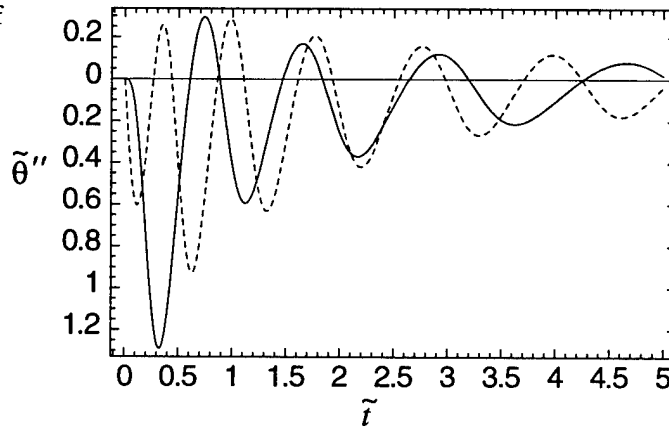
5. Conclusions

We have solved the dynamical equations (15), (16), and (23) for several different initial conditions (in addition to the ones discussed above) and with different values of the parameters. We have found that the dynamical behavior of the system can be very complex. In particular, the maximum current depends not only on the position of the rotor when the stator circuit switch is closed, but also on values of the stator circuit's resistance and inductance. Furthermore, the velocity of the launch package depends in a complicated way on the actual parameters in the problem. Consequently, it will also be profoundly affected by the characteristics of the field winding circuit, which was not included in our simplified model. In order to approach more closely the performance of a real EMRG, we are presently analyzing a model of an EMRG that includes a primary circuit. We will report our results and conclusions from that analysis in a future report.

Acknowledgments

18

References

1. S. C. Rashleigh and R. A. Marshall, "Electromagnetic Acceleration of Macroparticles to High Velocities," J. Appl. Phys. **49**, 2540 (1978).

2. P. Graneau, "Electromagnetic Jet-Propulsion in the Direction of Current Flow," Nature **295**, 311 (1982).

3. P. Graneau, "Compatibility of the Ampere and Lorentz Force Laws with the Virtual-Work Concept," Nuovo Cimento **78B**, 213 (1983).

4. P. T. Papas and P. G. Moyssides, "On the Fundamental Laws of Electrodynamics," Phys. Lett. **111A**, 193 (1985).

5. W. C. McCorkle, "Electromagnetic Gun (EMG) Report to the Deputy Undersecretary of the Army for Operations Research" (1997, manuscript in preparation).

6. L. D. Landau and E. M. Lifshitz, *Electrodynamics of Continuous Media*, Pergamon Press, New York (1960).

7. A. E. Fitzgerald, C. Kingsley, Jr., and S. D. Umans, *Electric Machinery*, fifth edition, McGraw-Hill, New York (1990).

Distribution

Admnstr
Defns Techl Info Ctr
Attn DTIC-OCP
8725 John J Kingman Rd Ste 0944
FT Belvoir VA 22060-6218

Ofc of the Dir Rsrch and Engrg
Attn R Menz
Pentagon Rm 3E1089
Washington DC 20301-3080

Ofc of the Secy of Defns
Attn ODDRE (R&AT) G Singley
Attn ODDRE (R&AT) S Gontarek
The Pentagon
Washington DC 20301-3080

OSD
Attn OUSD(A&T)/ODDDR&E(R) R Tru
Washington DC 20301-7100

CECOM
Attn PM GPS COL S Young
FT Monmouth NJ 07703

CECOM RDEC Elect System Div Dir
Attn J Niemela
FT Monmouth NJ 07703

CECOM
Sp & Terrestrial Commctn Div
Attn AMSEL-RD-ST-MC-M H Soicher
FT Monmouth NJ 07703-5203

Dir for MANPRINT
Ofc of the Deputy Chief of Staff for Prsnnl
Attn J Hiller
The Pentagon Rm 2C733
Washington DC 20301-0300

Dpty Assist Secy for Rsrch & Techl
Attn SARD-TT F Milton Rm 3E479
The Pentagon
Washington DC 20301-0103

Hdqtrs Dept of the Army
Attn DAMO-FDT D Schmidt
400 Army Pentagon Rm 3C514
Washington DC 20301-0460

MICOM RDEC
Attn AMSMI-RD W C McCorkle
Redstone Arsenal AL 35898-5240

US Army
CECOM Rsrch, Dev, & Engrg Ctr
Attn R F Giordano
FT Monmouth NJ 07703-5201

US Army Edgewood Rsrch, Dev, & Engrg Ctr
Attn SCBRD-TD J Vervier
Aberdeen Proving Ground MD 21010-5423

US Army Info Sys Engrg Cmnd
Attn ASQB-OTD F Jenia
FT Huachuca AZ 85613-5300

US Army Materiel Sys Analysis Agency
Attn AMXSY-D J McCarthy
Aberdeen Proving Ground MD 21005-5071

US Army Matl Cmnd
Dpty CG for RDE Hdqtrs
Attn AMCRD BG Beauchamp
5001 Eisenhower Ave
Alexandria VA 22333-0001

US Army Matl Cmnd
Prin Dpty for Acquisition Hdqrts
Attn AMCDCG-A D Adams
5001 Eisenhower Ave
Alexandria VA 22333-0001

US Army Matl Cmnd Prin
Dpty for Techlgy Hdqrts
Attn AMCDCG-T M Fisette
5001 Eisenhower Ave
Alexandria VA 22333-0001

US Army Mis Cmnd
Attn AMSAM-RD-WS-PL J Johnson
Redstone Arsenal AL 35898

US Army Natick Rsrch, Dev, & Engrg Ctr
Acting Techl Dir
Attn SSCNC-T P Brandler
Natick MA 01760-5002

US Army Rsrch Lab
Attn AMSRL-WT-P E Schmidt
Aberdeen Proving Ground MD 21005-5000

US Army Rsrch Ofc
Attn G Iafrate
4300 S Miami Blvd
Research Triangle Park NC 27709

US Army Simulation, Train, & Instrmntn
  Cmnd
Attn J Stahl
12350 Research Parkway
Orlando FL 32826-3726

US Army Tank-Automtv & Armaments Cmnd
Attn AMSTA-AR-TD C Spinelli
Bldg 1
Picatinny Arsenal NJ 07806-5000

US Army Tank-Automtv Cmnd
Rsrch, Dev, & Engrg Ctr
Attn AMSTA-TA J Chapin
Warren MI 48397-5000

US Army Test & Eval Cmnd
Attn R G Pollard III
Aberdeen Proving Ground MD 21005-5055

US Army Train & Doctrine Cmnd
Battle Lab Integration & Techl Dirctrt
Attn ATCD-B J A Klevecz
FT Monroe VA 23651-5850

US Military Academy
Dept of Mathematical Sci
Attn MAJ D Engen
West Point NY 10996

USAASA
Attn MOAS-AI W Parron
9325 Gunston Rd Ste N319
FT Belvoir VA 22060-5582

Nav Surface Warfare Ctr
Attn Code B07 J Pennella
17320 Dahlgren Rd Bldg 1470 Rm 1101
Dahlgren VA 22448-5100

GPS Joint Prog Ofc Dir
Attn COL J Clay
2435 Vela Way Ste 1613
Los Angeles AFB CA 90245-5500

DARPA
Attn B Kaspar
Attn L Stotts
3701 N Fairfax Dr
Arlington VA 22203-1714

ARL Electromag Group
Attn Campus Mail Code F0250 A Tucker
University of Texas
Austin TX 78712

The Univ of Texas at Austin
J J Pickle Rsrch Campus
Attn Mail Code R7000 A Walls
Attn Mail Code R7000 S Pratap
Center for Electromechanics
Austin TX 78712

Univ of Texas at Austin
Inst for Advanced Tech
Attn I Mcnab
4030-2 West Braker Ln
Austin TX 78759-5329

Palisades Inst for Rsrch Svc Inc
Attn E Carr
1745 Jefferson Davis Hwy Ste 500
Arlington VA 22202-3402

Sci Applications Internatl Corp
Attn W Rienstra
8200 N Mopac Expressway Ste 150
Austin TX 78759

Army Rsrch Lab
Attn AMSRL-WM I May
Aberdeen Proving Ground MD 21005-5000

US Army Rsrch Lab
Attn AMSRL-CI-LL Techl Lib (3 copies)
Attn AMSRL-CS-AL-TA Mail & Records
  Mgmt

Distribution (cont'd)

US Army Rsrch Lab (cont'd)
Attn AMSRL-CS-AL-TP Techl Pub (3 copies)
Attn AMSRL-D J Lyons
Attn AMSRL-SE D Wilmot
Attn AMSRL-SE J Pellegrino

US Army Rsrch Lab (cont'd)
Attn AMSRL-SE-EM D Wortman
Attn AMSRL-SE-EM T B Bahder (15 copies)
Adelphi MD 20783-1197

REPORT DOCUMENTATION PAGE			Form Approved OMB No. 0704-0188

Public reporting burden for this collection of information is estimated to average 1 hour per response, including the time for reviewing instructions, searching existing data sources, gathering and maintaining the data needed, and completing and reviewing the collection of information. Send comments regarding this burden estimate or any other aspect of this collection of information, including suggestions for reducing this burden, to Washington Headquarters Services, Directorate for Information Operations and Reports, 1215 Jefferson Davis Highway, Suite 1204, Arlington, VA 22202-4302, and to the Office of Management and Budget, Paperwork Reduction Project (0704-0188), Washington, DC 20503.

1. AGENCY USE ONLY (Leave blank)	2. REPORT DATE May 1998	3. REPORT TYPE AND DATES COVERED Interim, from Dec 1 1997 to Feb 27 1998

4. TITLE AND SUBTITLE Transient Response of an Electromagnetic Rail Gun: A Pedagogical Model	5. FUNDING NUMBERS PE: 61102A DA PR: AH47
6. AUTHOR(S) Thomas B. Bahder and John D. Bruno	

7. PERFORMING ORGANIZATION NAME(S) AND ADDRESS(ES) U.S. Army Research Laboratory Attn: AMSRL-SE-EP (bahder@arl.mil) 2800 Powder Mill Road Adelphi, MD 20783-1197	8. PERFORMING ORGANIZATION REPORT NUMBER ARL-TR-1663

9. SPONSORING/MONITORING AGENCY NAME(S) AND ADDRESS(ES) U.S. Army Research Laboratory 2800 Powder Mill Road Adelphi, MD 20783-1197	10. SPONSORING/MONITORING AGENCY REPORT NUMBER

12a. DISTRIBUTION/AVAILABILITY STATEMENT Approved for public release; distribution unlimited.	12b. DISTRIBUTION CODE

13. ABSTRACT (Maximum 200 words)

We present a highly simplified model of an electromagnetic rail gun. The energy source for the gun consists of a rotating magnetic dipole moment positioned at the center of a stator coil. The dipole moment is free to rotate about an axis normal to the stator coil's axis, inducing a current in the rail gun stator circuit, and thereby propelling the projectile. The system's dynamical behavior is described by three nonlinear coupled ordinary differential equations, involving time-dependent functions representing the armature's position, the stator circuit's current, and the dipole moment's angular position. We numerically solve this system of differential equations and plot the solutions versus time. The results exhibit a complicated dynamics due to the interaction of the electrical and mechnical degrees of freedom.

14. SUBJECT TERMS Electric gun, electromagnetic gun, rail gun, magnetic propulsion, physics, model			15. NUMBER OF PAGES 31
			16. PRICE CODE

17. SECURITY CLASSIFICATION OF REPORT Unclassified	18. SECURITY CLASSIFICATION OF THIS PAGE Unclassified	19. SECURITY CLASSIFICATION OF ABSTRACT Unclassified	20. LIMITATION OF ABSTRACT UL

NSN 7540-01-280-5500

Standard Form 298 (Rev. 2-89)
Prescribed by ANSI Std. Z39-18
298-102